Novel multiple tyrosine kinase inhibitor TAS-115 attenuates bleomycin-induced lung fibrosis in mice

Kazuya Koyama[1, 3], Hisatsugu Goto[1], Shun Morizumi[1], Kozo Kagawa[1], Haruka Nishimura[1], Seidai Sato[1], Hiroshi Kawano[1], Yuko Toyoda[1], Hirohisa Ogawa[2], Sakae Homma[3], Yasuhiko Nishioka[1]

Departments of [1]Respiratory Medicine and Rheumatology, [2]Molecular and Environmental Pathology, Graduate School of Biomedical Sciences, Tokushima University, Tokushima, Japan.

[3]Department of Respiratory Medicine, Toho University Graduate School of Medicine, Tokyo, Japan.

Contributions:

Conception and design: Kazuya Koyama, SS, HG, HK, YT, YN; Analysis and interpretation: SM, Kozo Kagawa, HN, HO; Drafting the manuscript for important intellectual content: HG, SH, YN

Address correspondence to: Yasuhiko Nishioka, Department of Respiratory Medicine and Rheumatology, Graduate School of Biomedical Sciences, Tokushima University, 3-18-15 Kuramoto-cho, Tokushima, Tokushima 770-8503, Japan.

Tel: +81-88-633-7127, Fax: +81-88-633-2134, E-mail: yasuhiko@tokushima-u.ac.jp

Running note: TAS-115 attenuates pulmonary fibrosis

Abstract

The signaling pathways of growth factors including platelet-derived growth factor (PDGF) can be considered specific targets for overcoming the poor prognosis of idiopathic pulmonary fibrosis (IPF). Nintedanib, the recently approved multiple kinase inhibitor, has shown promising anti-fibrotic effects in IPF patients; however, its efficacy is still limited, and in some cases, treatment discontinuation is necessary due to toxicities such as gastrointestinal disorders. Therefore, more effective agents with less toxicity are still needed. TAS-115 is a novel multiple tyrosine kinase inhibitor that preferably targets PDGF receptor (PDGFR), vascular endothelial growth factor receptor (VEGFR) and c-FMS in addition to other molecules. In this study, we evaluated the anti-fibrotic effect of TAS-115 on pulmonary fibrosis *in vitro* and *in vivo*. TAS-115 inhibited the phosphorylation of PDGFR on human lung fibroblast cell line MRC-5 cells and suppressed their PDGF-induced proliferation and migration. Furthermore, TAS-115 inhibited the phosphorylation of c-FMS, a receptor of macrophage colony-stimulating factor (M-CSF), in murine bone marrow-derived macrophages (BMDMs) and decreased the production of CCL2, another key molecule for inducing pulmonary fibrosis, under the stimulation of M-CSF. Importantly,

the inhibitory effects of TAS-115 on both PDGFR and c-FMS were 3- to 10-fold higher than those of nintedanib. In a mouse model of bleomycin-induced pulmonary fibrosis, TAS-115 significantly inhibited the development of pulmonary fibrosis and the collagen deposition in bleomycin-treated lungs. These data suggest that the strong inhibition of PDGFR and c-FMS by TAS-115 may be a promising strategy for overcoming the intractable pathogenesis of pulmonary fibrosis.

Key words: TAS-115; pulmonary fibrosis; platelet-derived growth factor receptor; c-FMS

Abbreviations:

IPF idiopathic pulmonary fibrosis

ECM extracellular matrix

PDGF platelet-derived growth factor

PDGFR PDGF receptor

FGF fibroblast growth factor

FGFR FGF receptor

VEGFR vascular endothelial growth factor receptor

CCL2 C-C motif chemokine ligand 2

M-CSF macrophage colony-stimulating factor

IC_{50} the half-maximal inhibitory concentration

α–SMA α-smooth muscle actin

BMDM bone marrow-derived macrophage

[^{3}H] thymidine deoxyribose ^{3}H-TdR

BAL bronchoalveolar lavage

BALF BAL fluid

BLM bleomycin

HGF hepatocyte growth factor

EMT epithelial-mesenchymal transition

TGF transforming growth factor

TNF tumor necrosis factor

IL interleukin

C_{max} maximum plasma concentration

$T_{1/2}$ half-life

Introduction

Idiopathic pulmonary fibrosis (IPF) is a life-threatening and chronic progressive fibrotic lung disease (1). Its pathological findings are characterized by excessive accumulation of extracellular matrix (ECM) and irreversible destruction of lung architecture. Although its detailed etiology is unknown, lung epithelial damage and subsequent excessive production of ECM, including collagen fibers, are considered clues to help understanding the disease behavior. Since these pathogeneses are regulated by a variety of growth factors, targeting those molecules is suggested to be a promising strategy for treating patients with pulmonary fibrosis.

Among the growth factors involved in the pathogenesis of pulmonary fibrosis, we have previously shown that the platelet-derived growth factor (PDGF)-PDGF receptor (PDGFR) axis plays a crucial role in lung fibrosis in mice by enhancing the proliferation and migration of fibroblasts and fibrocytes (2-5). We demonstrated that the multiple kinase inhibitor imatinib mesylate, a drug originally developed to treat chronic myeloid leukemia by targeting BCR-ABL, possessed an anti-fibrotic effect by suppressing PDGF signaling (4, 5). Although the results of the clinical trial assessing the anti-fibrotic effect of imatinib on IPF were negative (6), the significance of the

blockade of growth factor signaling on pulmonary fibrosis was recently demonstrated by clinical trials using nintedanib, which also targets multiple kinases, including PDGFR (7). The results showed that nintedanib reduced the decline in the respiratory function compared with placebo treatment in IPF patients. The difference between the results of imatinib and nintedanib trials may be partly explained by differences in their inhibitory activities against PDGFR phosphorylation. The inhibitory effect of nintedanib on PDGF signaling is approximately 10-fold stronger than that of imatinib (8). However, whether or not nintedanib improves the survival of IPF patients remains unclear, suggesting that treatment with nintedanib is still insufficient to overcome the intractable pathogenesis of pulmonary fibrosis. Furthermore, nintedanib often causes toxicities, such as gastrointestinal disorders, that can result in treatment discontinuation. Therefore, further efforts are needed to develop more selective and effective agents with less toxicity that target growth factor signaling in order to improve the prognosis of patients with pulmonary fibrosis.

TAS-115 is an oral tyrosine kinase inhibitor that suppresses the phosphorylation of PDGFR, vascular endothelial growth factor recetor (VEGFR), c-FMS and MET (9, 10). A previous study using murine tumor models showed that the phosphorylation of

PDGFR was suppressed with TAS-115 at less than 10 nM, which was lower than the corresponding concentration of nintedanib (the IC_{50} of nintedanib for PDGFRα and β was reported as 59 and 65 nM, respectively) (9, 11), suggesting that TAS-115 might also be useful as an anti-fibrotic drug. Furthermore, in addition to the blockade of PDGFR, TAS-115 inhibits macrophage colony-stimulating factor (M-CSF) signaling by inhibiting the phosphorylation of c-FMS, a receptor of M-CSF. M-CSF was reported to be involved in lung fibrotic change in mouse models by the induction of C-C motif chemokine ligand 2 (CCL2) (12), which is a key chemoattractant for fibrocytes (13). These results suggest that TAS-115 may exert favorable effects on pulmonary fibrosis by targeting the M-CSF-CCL2 axis in addition to PDGFR.

At present, the pharmacological activity and preferable potency of TAS-115 to inhibit PDGFR and c-FMS have been shown only in tumor models (9, 10). We therefore hypothesized that TAS-115 also effectively attenuates lung fibrosis by inhibiting the phosphorylation of PDGFR and c-FMS. To assess this hypothesis, we conducted *in vitro* and *in vivo* studies to evaluate the effect of TAS-115 on pulmonary fibrosis and assessed its usefulness compared to nintedanib.

Materials and Methods

The detailed methods are described in the online supplementary materials.

Mice and agents

Eight-week-old C57BL/6 male mice were purchased from Charles River Japan Inc. (Tokyo, Japan) The mice were maintained in the animal facility of the Tokushima University according to the guidelines of Tokushima University (4). All experimental protocols were approved by the animal research committee of Tokuhsima University. TAS-115 was provided by Taiho Pharmaceutical (Tokyo, Japan). Nintedanib and bleomycin were purchased from Chemscene (Monmouth Junction, NJ, USA) and Nippon Kayaku Co. (Tokyo, Japan), respectively. Recombinant human cytokines including PDGF-BB, M-CSF and transforming growth factor-β (TGF-β) were purchased from R&D Systems (Minneapolis, MN, USA). Antibodies for PDGFRβ, phosphor-PDGFRα/β, c-FMS, phospho-c-FMS were purchased from Cell Signaling Technology (Danvers, MA, USA). Anti-collagen 1 antibody was purchased from Abcam (Cambridge, MA, USA). Anti-α smooth muscle actin (α–SMA) antibody was purchased from Sigma-Aldrich (St. Louis, MO, USA). Anti-actin β was purchased

from Santa Cruz Biotechnology (Santa. Cruz, CA, USA). MRC-5 cells were purchased from DS PHARMA BIOMEDICAL (Osaka, Japan). Murine lung fibroblasts were isolated according to the method reported previously (14). Bone marrow-derived macrophages (BMDMs) were obtained from mice as previously described (12).

Half-maximal inhibitory concentration (IC_{50})

Enzyme inhibition studies were performed using a mobility shift assay.

Analyses of the expression of proteins

Immunoblotting was performed to assess the expression of proteins and the phosphorylation of PDGFR (15). Simple Western^{TM} System (ProteinSimple, Santa Clara, CA, USA) was used to determine the phosphorylation of c-FMS.

Cell proliferation assay

A [^{3}H] thymidine deoxyribose (^{3}H-TdR) incorporation assay was performed to assess the proliferation of the fibroblasts.

Cell migration assay

The migration of fibroblasts was evaluated using a trans-well cell migration assay.

qRT-PCR

RT-PCR was performed as previously described (16). The sequences of primers were described in the online supplementary materials.

Measurement of cytokine concentrations

Concentrations of CCL2 and M-CSF were examined with an enzyme-linked immunosorbent assay (ELISA) kit (R&D Systems). The concentrations of the other cytokines were measured by Bio-Plex assay (Bio-Rad Laboratories, Hercules, CA, USA).

Bleomycin-induced pulmonary fibrosis in mice

The mice received a single transbronchial instillation of 3.0 mg/kg BLM on day 0. TAS-115, nintedanib or distilled water was administered daily by gavage from day 0.

The dosage of TAS-115 was 30mg/kg or 100mg/kg that was determined based on previous study evaluating its anti-tumor effect *in vivo* (9).

BAL

BAL was performed with saline (1 ml) using a soft cannula. After counting the cell numbers in the BAL fluid (BALF), cells were stained with Diff-Quick for cell classification (2).

Hydroxyproline assay

The hydroxyproline contents of the BLM-treated lungs were measured using a Hydroxyproline Colorimetric Assay kit (BioVision, Milpitas, CA, USA).

Histopathology

Murine lungs were embedded in paraffin, and the sections were stained with hematoxylin-eosin stain and Azan Mallory staining. The fibrotic changes were evaluated by the Ashcroft score (17).

Statistical analyses

The significance of differences was analyzed using the one-way ANOVA, followed by Tukey's multiple-comparison post-hoc test. p values of less than 0.05 were considered to be significant.

Results

Inhibitory activities of TAS-115 on growth factor receptors

Enzyme inhibition studies were performed to determine the IC_{50} of TAS-115 on PDGFRα, PDGFRβ, VEGFR1-2, c-FMS and fibroblast growth factor receptor (FGFR)1-3. The evaluated values of IC_{50} were shown in Table 1. TAS-115 inhibited the phosphorylation of PDGFRα, PDGFRβ, VEGFR1, VEGFR2 and c-FMS effectively. In contrast, the IC_{50} values of TAS-115 against FGFRs were relatively high.

TAS-115 suppresses the proliferation and migration of fibroblasts via the inhibition of PDGFR signaling

We evaluated the effect of TAS-115 on the phosphorylation of PDGFR in human fibroblast MRC-5 cells (Figure 1A and B). TAS-115 inhibited the phosphorylation of PDGFR in a dose-dependent manner, and its inhibitory effect was observed at 3 nM, which was lower than that of nintedanib. We then examined whether or not TAS-115 affected fibroblasts' biological responses to PDGF-BB treatment using a ^{3}H-TdR incorporation assay and trans-well migration assay (Figure 1C and D). The ^{3}H-TdR

incorporation assay showed that TAS-115 inhibited the PDGF-BB-induced proliferation of MRC-5 cells in a dose-dependent manner (Figure 1C). In addition, the trans-well migration assay showed that TAS-115 suppressed the PDGF-BB-induced migration of MRC-5 cells in a dose-dependent manner (Figure 1D). Of note, TAS-115 suppressed the proliferation of MRC-5 cells at 3nM and migration of cells at 1 nM, although nintedanib failed to inhibit the migration at the same concentration. Similar effects of TAS-115 on PDGFR phosphorylation, cell proliferation and cell migration were observed in murine primary lung fibroblasts (Figure E1). These data indicated that TAS-115 inhibited the phosphorylation of PDGFR and suppressed the biological activities of fibroblasts more effectively than nintedanib.

The production of ECM and α-SMA, which are strongly induced by TGF-β stimulation, is the hallmark of pulmonary fibrosis (13). We next explored if TAS-115 had an activity to suppress TGF-β-stimulated expression of collagen 1 and α-SMA in MRC-5 cells (Figure E2). The results indicated that TAS-115 as well as nintedanib did not suppress the production of collagen 1 or α-SMA.

TAS-115 inhibits phosphorylation of c-FMS

TAS-115 was reported to inhibit the phosphorylation of c-FMS in tumor cells (10, 18). We investigated the effect of this compound on M-CSF-induced c-FMS phosphorylation in BMDMs compared with nintedanib. TAS-115 inhibited the tyrosine phosphorylation of c-FMS at 10 nM, whereas 100 nM or more was needed for nintedanib to express the similar inhibitory effects (Figure 2A, B). These results indicated that TAS-115 effectively suppressed the phosphorylation of c-FMS compared to nintedanib.

TAS-115 suppresses CCL2 production in vitro and in vivo via the blockade of the M-CSF-c-FMS axis

Induction of CCL2 expression by the M-CSF-c-FMS axis contributes to the fibrotic changes in the lungs (12). CCL2 has been reported to be produced in the damaged lung (12, 19), and it regulates the recruitment and activation of fibrocytes and fibroblasts that express C-C chemokine receptor type 2 (13, 20-22). One of the anti-fibrotic activities of pirfenidone, another clinically approved anti-fibrotic drug, is considered to be the inhibition of the migration of fibrocytes via the suppression of CCL2 production (23). Therefore, we hypothesized that the inhibition of the

phosphorylation of c-FMS by TAS-115 decreases the CCL2 production in the lungs and thereby attenuates the fibrotic process. To confirm this, we evaluated whether or not TAS-115 inhibits the M-CSF-dependent CCL2 production in BMDMs *in vitro*. As expected, M-CSF stimulation increased the CCL2 production of BMDMs, and TAS-115 effectively inhibited the CCL2 production at a lower dose than nintedanib (Figure 3A).

We next assessed the inhibitory effect of TAS-115 on the M-CSF-CCL2 axis in BLM-induced murine pulmonary fibrosis. TAS-115, nintedanib or vehicle was administered for 3 days starting at 7 days after BLM treatment, and then the BALF was collected and analyzed to assess the CCL2 or M-CSF concentration (Figure 3B). The concentration of CCL2 in the BALF was increased by BLM treatment, which was consistent to the previous reports using mouse model of infectious or non-infectious lung injury (12, 19). Administration of TAS-115 significantly reduced the concentration of CCL2 (Figure 3C) without affecting M-CSF concentration (Figure 3D). Meanwhile, treatment with nintedanib failed to suppress CCL2 expression. These results indicate that TAS-115 has a potent effect on inhibiting M-CSF-CCL2 axis, but not MCSF production, and this characteristic is not found in the pharmacodynamics of

nintedanib *in vivo*.

TAS-115 attenuates bleomycin-induced lung fibrosis

To examine the anti-fibrotic effect of TAS-115 *in vivo*, we used a mouse model of BLM-induced pulmonary fibrosis. After receiving a single transbronchial instillation of 3.0 mg/kg BLM, the mice were treated daily with TAS-115 (30 or 100 mg/kg/day), nintedanib (60 mg/kg/day) or vehicle from day 0. On day 21, the mice were killed, and the fibrotic changes in the lungs were assessed using the Ashcroft scoring system and a hydroxyproline assay. The histological findings of the lungs showed that the BLM treatment induced inflammatory and fibrotic changes leading to an increased Ashcroft score and hydroxyproline content (Figure 4). The administration of TAS-115 significantly inhibited the histological changes and decreased both the Ashcroft score and hydroxyproline content at a dose of 30 mg/kg. A similar effect was observed when the mice were treated with nintedanib at 60 mg/kg.

Anti-fibrotic agents including nintedanib were reported to reduce the number of inflammatory cells and inflammatory cytokines in BALF of BLM-treated mice (24-26). Therefore we next examined the cell counts and the cytokine profiles in the BALF

collected at 7, 14 and 21 days after BLM instillation (Figure 5, E3, E4). At both 14 and 21 days after BLM treatment, the concentration of TGF-β was lower in the TAS-115-treated group (100 mg/kg/day) than in the nintedanib-treated group (Figure 5, E4B). Referring to the levels of inflammatory cytokines, TAS-115 more effectively inhibited the production of tumor necrosis factor (TNF)-α than nintedanib, although the inhibitory effects of TAS-115 and nintedanib on interleukin (IL)-6 and interferon (IFN)-γ production were similar (Figure 5, E4B). The inflammatory cell counts in the BALF showed that both tyrosine kinase inhibitors decreased the numbers of lymphocytes at the both day 14 and 21 as previously indicated in the experiment using nintedanib (Figure 5, E4A) (24). On day 7, there were no differences in cytokine profile and cell numbers by TAS-115 or nintedanib treatment (Figure E3). These data indicated that TAS-115 effectively suppressed pro-inflammatory and pro-fibrotic cytokines contributing to lung fibrosis in the fibrotic phase.

Discussion

In the present study, we investigated the antifibrotic effects of a novel multiple tyrosine kinase inhibitor TAS-115. TAS-115 clearly showed the higher inhibitory activities on the phosphorylation of both PDGFR and c-FMS than nintedanib. The migration and proliferation of lung fibroblasts mediated by PDGF and the CCL2 production of macrophages induced by M-CSF were more strongly inhibited by TAS-115 as compared to nintedanib. The *in vivo* antifibrotic effects of TAS-115 were also demonstrated in BLM-induced pulmonary fibrosis model.

Among several growth factors, PDGF-PDGFR axis has been consistently reported to play important roles in suppressing lung fibrotic change by reducing the proliferation and migration of fibroblasts (2-4, 27, 28). In this study, TAS-115 showed lower IC_{50} values against PDGFRα/β (IC_{50}=0.81±0.10/7.06±0.83 nM), nearly almost equal values for VEGFR2 (IC_{50}=30±9 nM) and higher values for FGFR1 (IC_{50}>970 nM), FGFR2 (IC_{50}=340±130 nM), and FGFR3 (IC_{50}>940 nM), compared with the previously reported IC_{50} values of nintedanib (PDGFRα/β 59±71/65±7 nM, VEGFR2 21±13 nM, FGFR1/2/3 69±70/37±2/108±41 nM) (11, 29). These data suggests that TAS-115 strongly suppresses PDGF signaling in the local lung microenvironment and

therefore may be a promising anti-fibrotic agent against IPF.

The roles of VEGFR and FGFR, the other molecules targeted by nintedanib, in pulmonary fibrosis are controversial. For instance, a VEGFR antagonist was reported to attenuate BLM-induced lung fibrosis in mice (30). Cao et al. reported that VEGFR1-expressing macrophages enhance lung fibrotic change by stimulating Notch signaling in fibroblasts (31). In a clinical study, Barratt et al. showed that the VEGF-A splice variant affects the development of pulmonary fibrosis (32). These findings suggest the pro-fibrotic role of VEGF in pulmonary fibrosis. However, Murray et al. recently reported the protective role of VEGF during pulmonary fibrosis by modulating epithelial homeostasis (33). Although we could not assess the effect of TAS-115 on VEGF/VEGFR signaling in lung fibroblasts because the cell line we used (MRC-5 cells) did not express VEGFR, the further study using primary fibroblasts and animal models would be required. In terms of the FGF-FGFR axis, the blockade of FGF signaling may show an anti-fibrotic effect via the inhibition of the proliferation of fibroblasts (34). However, it may also worsen the excessive fibrotic changes in the lung by mechanisms such as the inhibition of epithelial repair (35-37). Furthermore, some FGFs, such as FGF1, have shown anti-fibrotic activities, including the inhibition

of epithelial-mesenchymal transition (EMT), myofibroblast differentiation and collagen production of fibroblasts (35, 38, 39). These results suggest that VEGF and FGF regulate the process of pulmonary fibrosis through diverse mechanisms and can be both pro- and anti-fibrotic. As such, careful attention is needed when developing anti-fibrotic agents that target these molecules. In this study, we showed that the IC_{50} value of TAS-115 for FGFR was higher than that of nintedanib, suggesting that TAS-115 may have a stronger anti-fibrotic effect.

Another considerable advantage of TAS-115 as an anti-fibrotic agent is that TAS-115 suppresses the phosphorylation of c-FMS more effectively than nintedanib. Although the data of precise IC_{50} of nintedanib for c-FMS has not been referred in previous article, Tandon et al. showed that inhibited the phosphorylation of c-FMS at the concentration of 300nM (40). Together with our results, it is suggested that the IC_{50} of TAS-115 against c-FMS is lower compared with that of nintedanib. Regarding the significance of M-CSF in pulmonary fibrosis, Baran et al. reported that M-CSF aggravated fibrogenesis by inducing CCL2 production in the lung (12). This M-CSF-CCL2 axis may be a potential treatment target, and TAS-115 has potency for attenuating lung fibrosis via c-FMS blockade, resulting in the reduction of CCL2

expression.

TAS-115 also differs from nintedanib with regard to its suppressive effect against hepatocyte growth factor (HGF) signaling. Similar to nintedanib, TAS-115 was originally designed as a multi-tyrosine kinase inhibitor against cancer by targeting VEGFR, EGFR and HGF receptor (MET) (10, 18, 41). Thus, this drug was expected to have therapeutic potential against cancer, especially those with bone metastasis and acquired resistance to cytotoxic agents by MET amplification. However, previous reports have indicated that enhanced HGF/MET signaling with HGF protein or gene transfer has a protective role in the pathogenesis of pulmonary fibrosis (42-45). Although the physiological role of HGF in the fibrogenesis of the lungs is still unclear, targeting MET may exacerbate pulmonary fibrosis. In the present study, TAS-115 exerted a significant anti-fibrotic effect, possibly due to the strong inhibition of PDGFR and c-FMS, and eliminating MET from the target might further enhance the efficacy of this drug.

Our study showed that TAS-115 attenuated BLM-induced lung fibrosis as we expected based on its profile of kinase inhibition. BALF examinations revealed that TAS-115 reduced the lymphocyte count and concentrations of pro-inflammatory and

pro-fibrotic cytokines in the fibrotic phase of BLM-treated mice, not in acute inflammation phase. This phenomenon is consistent with our observation previously shown in antifibrotic effects of imatinib(4) and previous experiment assessing the anti-fibrotic effect of nintedanib (24), and is considered to be the reflection of suppression of inflammation related to fibrotic change. Specifically, TAS-115 effectively suppressed the TNF-α and TGF-β expression more strongly than nintedanib (Figure 6). Because those cytokines are known to play critical roles in pulmonary fibrosis (46, 47), the favorable effect of TAS-115 on the TNF-α and TGF-β expression further supports the usefulness of TAS-115 as an anti-fibrotic agent for pulmonary fibrosis. The expression of IL-6 was also inhibited in both tyrosine kinase inhibitor-treated groups, although the level of suppressive effects of TAS-115 and nintedanib on IL-6 was variable between days 14 and 21, suggesting that these tyrosine kinase inhibitors affect late phase inflammation related to fibrotic change, although they did not inhibit acute inflammation on day 7.

In terms of its safety, the results from a phase 1 study of TAS-115 in solid tumors revealed its good clinical tolerability, including a low frequency of severe diarrhea (Grade 1-2: 14.3%, Grade 3-4: 0%) (48), which is known to be a common

problematic side effect of nintedanib (all grades: 62.4%) (7). In addition, TAS-115 has better bioavailability than nintedanib (maximum plasma concentration at 200 mg/day: TAS-115 2500-3000 ng/ml vs. nintedanib 30-50 ng/ml) (44-46), suggesting that TAS-115 would effectively suppress the targeted receptors in patients with IPF.

In conclusion, TAS-115 has a preferable kinase inhibition profile that suppresses the PDGFR and c-FMS signaling pathways and attenuates BLM-induced lung fibrosis in mice. TAS-115 may be a new effective multiple kinase inhibitor for treating patients with pulmonary fibrosis via the strong inhibition of target molecules with favorable bioavailability. In the near future, the anti-fibrotic effects of TAS-115 will be demonstrated by ongoing phase II clinical trial to evaluate the efficacy and safety for patients with IPF.

Acknowledgement

We thank Ms. Tomoko Oka for her technical assistance and the members of Nishioka lab for their technical advice and useful discussion. This research was supported in part by the Practical Research Project for Rare Intractable Diseases from the Japan Agency for Medical Research and Development (AMED) and by grants from the Ministry of Health, Labour and Welfare, Japan awarded to the Study Group on Diffuse Pulmonary Disorders, Scientific Research/Research on Intractable Diseases and from Taiho Pharmaceutical (Y.N.).

Table 1. Kinase inhibition profile of TAS-115.

Kinase	IC_{50} (nM)
PDGFRα	0.81±0.10
PDGFRβ	7.06±0.83
VEGFR1	140±40
VEGFR2	30±9*
FGFR1	>970
FGFR2	340±130
FGFR3	>940
c-FMS	15*

*From the data published in Ref. 10.

Figure Legends

Figure 1.

TAS-115 inhibits the phosphorylation of PDGFR on MRC-5 cells and suppresses the PDGF-induced proliferation and migration. (A) Human lung fibroblast cell line MRC-5 cells were incubated with PDGF-BB (100 ng/ml) with or without different concentrations (0-1000 nM) of TAS-115 or nintedanib. The phosphorylation of PDGFR was analyzed by immunoblotting. (B) Relative intensities of the bands of phosphorylated PDGFRα/β to PDGFRβ are shown. The intensities were determined using a National Institutes of Health imaging program (n=3). (C) The proliferation of MRC-5 cells was measured by a ^{3}H-TdR incorporation assay (n=4). MRC-5 cells were incubated with PDGF-BB (100 ng/ml) with or without different concentrations (0-100 nM) of TAS-115 or nintedanib. (D) The migration of MRC-5 cells was assessed by a trans-well migration assay (n=3). Fibroblasts plated on the upper chamber with a pore size of 8 μm were stimulated with PDGF-BB (100 ng/ml) added to the lower chamber. The indicated concentrations of TAS-115 or nintedanib were added to the upper chamber to assess their effect on cell migration. After 24 h, the number of fibroblasts that had migrated to the bottom surface of the filter was counted. *$p<0.05$ versus groups treated with PDGF-BB without TAS-115 or nintedanib.

**p<0.005 versus groups treated with PDGF-BB without TAS-115 or nintedanib. ***p<0.001 versus groups treated with PDGF-BB without TAS-115 or nintedanib.

Figure 2.

TAS-115 inhibits the phosphorylation of c-FMS on murine BMDMs. (A) BMDMs were incubated with M-CSF (100 ng/ml) with or without the indicated concentration (0-1000 nM) of TAS-115 or nintedanib. The phosphorylation of c-FMS was determined by a Simple Western^{TM} System. (B) The relative intensity of phosphorylated c-FMS to c-FMS is shown (n=3). *p<0.01 versus groups treated with M-CSF without TAS-115 or nintedanib.

Figure 3.

TAS-115 suppresses M-CSF-induced c-FMS production by BMDMs. (A) MCSF (100 ng/ml)-stimulated BMDMs were cultured with the indicated concentration of TAS-115 or nintedanib for 24 h (n=4). The concentration of CCL2 in the culture supernatant was measured by an ELISA. *p<0.001 versus groups treated with PDGF-BB without TAS-115 or nintedanib. (B) TAS-115 (100 mg/kg/day), nintedanib

(60 mg/kg/day) or vehicle was administered for 3 days starting at 7 days after a single transbronchial instillation of 3.0 mg/kg BLM. On day 10, the mice were killed, and the BALF was collected for further analyses (n=6). (C)(D) The concentrations of CCL2 and M-CSF in the BALF were determined by an ELISA. *p<0.05. **p<0.01 ***p<0.001.

Figure 4.

TAS-115 attenuates BLM-induced lung fibrosis. Mice received a single transbronchial instillation of 3.0 mg/kg BLM on day 0, and TAS-115 (30 or 100 mg/kg/day), nintedanib (60 mg/kg/day) or vehicle was administered daily from day 0. Mice were killed, and the lungs were collected on day 21. Lung sections were stained with (A) hematoxylin and eosin (H&E) stain or (B) azan Mallory. (C) The fibrotic changes in the lungs were quantified with a numerical fibrotic score (Ashcroft score) histopathologically (n=6). (D) Lungs were homogenized in distilled water, and the hydroxyproline contents were measured by a hydroxyproline assay (n=6). *p<0.05 versus groups treated with BLM without TAS-115 or nintedanib. **p<0.01 versus groups treated with BLM without TAS-115 or nintedanib. ***p<0.001 versus groups

treated with BLM without TAS-115 or nintedanib.

Figure 5.

The assessment of the cell counts (A) and cytokine expression (B) in the BALF of BLM-treated mice. Mice received a single transbronchial instillation of 3.0 mg/kg BLM on day 0, and TAS-115 (30 or 100 mg/kg/day), nintedanib (60 mg/kg/day) or vehicle was administered daily from day 0. Mice were killed, and the BALF was collected on day 14 (n=6). *p<0.05 versus groups treated with BLM without TAS-115 or nintedanib. **p<0.01 versus groups treated with BLM without TAS-115 or nintedanib. ***p<0.001 versus groups treated with BLM without TAS-115 or nintedanib.

References

1. Raghu G, Collard HR, Egan JJ, Martinez FJ, Behr J, Brown KK, Colby TV, Cordier JF, Flaherty KR, Lasky JA, et al. An official ats/ers/jrs/alat statement: Idiopathic pulmonary fibrosis: Evidence-based guidelines for diagnosis and management. *Am J Respir Crit Care Med* 2011;183(6):788-824.

2. Aono Y, Kishi M, Yokota Y, Azuma M, Kinoshita K, Takezaki A, Sato S, Kawano H, Kishi J, Goto H, et al. Role of platelet-derived growth factor/platelet-derived growth factor receptor axis in the trafficking of circulating fibrocytes in pulmonary fibrosis. *Am J Respir Cell Mol Biol* 2014;51(6):793-801.

3. Nishioka Y, Azuma M, Kishi M, Aono Y. Targeting platelet-derived growth factor as a therapeutic approach in pulmonary fibrosis. *J Med Invest* 2013;60(3-4):175-183.

4. Aono Y, Nishioka Y, Inayama M, Ugai M, Kishi J, Uehara H, Izumi K, Sone S. Imatinib as a novel antifibrotic agent in bleomycin-induced pulmonary fibrosis in mice. *Am J Respir Crit Care Med* 2005;171(11):1279-1285.

5. Azuma M, Nishioka Y, Aono Y, Inayama M, Makino H, Kishi J, Shono M, Kinoshita K, Uehara H, Ogushi F, et al. Role of α1-acid glycoprotein in

therapeutic antifibrotic effects of imatinib with macrolides in mice. *Am J Respir Crit Care Med* 2007;176(12):1243-1250.

6. Daniels CE, Lasky JA, Limper AH, Mieras K, Gabor E, Schroeder DR, Imatinib IPFSI. Imatinib treatment for idiopathic pulmonary fibrosis: Randomized placebo-controlled trial results. *Am J Respir Crit Care Med* 2010;181(6):604-610.

7. Richeldi L, du Bois RM, Raghu G, Azuma A, Brown KK, Costabel U, Cottin V, Flaherty KR, Hansell DM, Inoue Y, et al. Efficacy and safety of nintedanib in idiopathic pulmonary fibrosis. *N Engl J Med* 2014;370(22):2071-2082.

8. Hilberg F, Tontsch-Grunt U, Baum A, Le AT, Doebele RC, Lieb S, Gianni D, Voss T, Garin-Chesa P, Haslinger C, et al. The triple angiokinase inhibitor nintedanib directly inhibits tumor cell growth and induces tumor shrinkage via blocking oncogenic receptor tyrosine kinases. *J Pharmacol Exp Ther* 2017.

9. Yamada S, Imura Y, Nakai T, Nakai S, Yasuda N, Kaneko K, Outani H, Takenaka S, Hamada K, Myoui A, et al. Therapeutic potential of TAS-115 via c-MET and PDGFRα signal inhibition for synovial sarcoma. *BMC Cancer* 2017;17(1):334.

10. Fujita H, Gomori A, Fujioka Y, Kataoka Y, Tanaka K, Hashimoto A, Suzuki T, Ito K, Haruma T, Yamamoto-Yokoi H, et al. High potency vegfrs/met/fms triple blockade by TAS-115 concomitantly suppresses tumor progression and bone destruction in tumor-induced bone disease model with lung carcinoma cells. *PLoS One* 2016;11(10):e0164830.

11. Hilberg F, Roth GJ, Krssak M, Kautschitsch S, Sommergruber W, Tontsch-Grunt U, Garin-Chesa P, Bader G, Zoephel A, Quant J, et al. BIBF 1120: Triple angiokinase inhibitor with sustained receptor blockade and good antitumor efficacy. *Cancer Res* 2008;68(12):4774-4782.

12. Baran CP, Opalek JM, McMaken S, Newland CA, O'Brien JM, Jr., Hunter MG, Bringardner BD, Monick MM, Brigstock DR, Stromberg PC, et al. Important roles for macrophage colony-stimulating factor, CC chemokine ligand 2, and mononuclear phagocytes in the pathogenesis of pulmonary fibrosis. *Am J Respir Crit Care Med* 2007;176(1):78-89.

13. Wolters PJ, Collard HR, Jones KD. Pathogenesis of idiopathic pulmonary fibrosis. *Annu Rev Pathol* 2014;9:157-179.

14. Phan SH, Varani J, Smith D. Rat lung fibroblast collagen metabolism in

bleomycin-induced pulmonary fibrosis. *J Clin Invest* 1985;76(1):241-247.

15. Mitani K, Nishioka Y, Yamabe K, Ogawa H, Miki T, Yanagawa H, Sone S. Soluble Fas in malignant pleural effusion and its expression in lung cancer cells. *Cancer Sci* 2003;94(3):302-307.

16. Mitsuhashi A, Goto H, Saijo A, Trung VT, Aono Y, Ogino H, Kuramoto T, Tabata S, Uehara H, Izumi K, et al. Fibrocyte-like cells mediate acquired resistance to anti-angiogenic therapy with bevacizumab. *Nat Commun* 2015;6:8792.

17. Ashcroft T, Simpson JM, Timbrell V. Simple method of estimating severity of pulmonary fibrosis on a numerical scale. *J Clin Pathol* 1988;41(4):467-470.

18. Watanabe K, Hirata M, Tominari T, Matsumoto C, Fujita H, Yonekura K, Murphy G, Nagase H, Miyaura C, Inada M. The MET/vascular endothelial growth factor receptor (VEGFR)-targeted tyrosine kinase inhibitor also attenuates fms-dependent osteoclast differentiation and bone destruction induced by prostate cancer. *J Biol Chem* 2016;291(40):20891-20899.

19. Lai C, Wang K, Zhao Z, Zhang L, Gu H, Yang P, Wang X. C-C motif chemokine ligand 2 (CCL2) mediates acute lung injury induced by lethal influenza H7N9 virus. *Front Microbiol* 2017;8:587.

20. Ekert JE, Murray LA, Das AM, Sheng H, Giles-Komar J, Rycyzyn MA. Chemokine (C-C motif) ligand 2 mediates direct and indirect fibrotic responses in human and murine cultured fibrocytes. *Fibrogenesis Tissue Repair* 2011;4(1):23.

21. Liu X, Das AM, Seideman J, Griswold D, Afuh CN, Kobayashi T, Abe S, Fang Q, Hashimoto M, Kim H, et al. The CC chemokine ligand 2 (CCL2) mediates fibroblast survival through IL-6. *Am J Respir Cell Mol Biol* 2007;37(1):121-128.

22. Moore BB, Kolodsick JE, Thannickal VJ, Cooke K, Moore TA, Hogaboam C, Wilke CA, Toews GB. CCR2-mediated recruitment of fibrocytes to the alveolar space after fibrotic injury. *Am J Pathol* 2005;166(3):675-684.

23. Inomata M, Kamio K, Azuma A, Matsuda K, Kokuho N, Miura Y, Hayashi H, Nei T, Fujita K, Saito Y, et al. Pirfenidone inhibits fibrocyte accumulation in the lungs in bleomycin-induced murine pulmonary fibrosis. *Respir Res* 2014;15:16.

24. Wollin L, Maillet I, Quesniaux V, Holweg A, Ryffel B. Antifibrotic and anti-inflammatory activity of the tyrosine kinase inhibitor nintedanib in experimental models of lung fibrosis. *J Pharmacol Exp Ther* 2014;349(2):209-220.

25. Liu Y, Lu F, Kang L, Wang Z, Wang Y. Pirfenidone attenuates bleomycin-induced pulmonary fibrosis in mice by regulating Nrf2/Bach1 equilibrium. *BMC Pulm Med* 2017;17(1):63.

26. Li LF, Kao KC, Liu YY, Lin CW, Chen NH, Lee CS, Wang CW, Yang CT. Nintedanib reduces ventilation-augmented bleomycin-induced epithelial-mesenchymal transition and lung fibrosis through suppression of the Src pathway. *J Cell Mol Med* 2017;21(11):2937-2949.

27. Inomata M, Nishioka Y, Azuma A. Nintedanib: Evidence for its therapeutic potential in idiopathic pulmonary fibrosis. *Core Evid* 2015;10:89-98.

28. Rice AB, Moomaw CR, Morgan DL, Bonner JC. Specific inhibitors of platelet-derived growth factor or epidermal growth factor receptor tyrosine kinase reduce pulmonary fibrosis in rats. *Am J Pathol* 1999;155(1):213-221.

29. Kanaan R, Strange C. Use of multitarget tyrosine kinase inhibitors to attenuate platelet-derived growth factor signalling in lung disease. *Eur Respir Rev* 2017;26(146).

30. Ou XM, Li WC, Liu DS, Li YP, Wen FQ, Feng YL, Zhang SF, Huang XY, Wang T, Wang K, et al. VEGFR-2 antagonist SU5416 attenuates bleomycin-induced

pulmonary fibrosis in mice. *Int Immunopharmacol* 2009;9(1):70-79.

31. Cao Z, Lis R, Ginsberg M, Chavez D, Shido K, Rabbany SY, Fong GH, Sakmar TP, Rafii S, Ding BS. Targeting of the pulmonary capillary vascular niche promotes lung alveolar repair and ameliorates fibrosis. *Nat Med* 2016;22(2):154-162.

32. Barratt SL, Blythe T, Jarrett C, Ourradi K, Shelley-Fraser G, Day MJ, Qiu Y, Harper S, Maher TM, Oltean S, et al. Differential expression of VEGF-Axxx isoforms is critical for development of pulmonary fibrosis. *Am J Respir Crit Care Med* 2017;196(4):479-493.

33. Murray LA, Habiel DM, Hohmann M, Camelo A, Shang H, Zhou Y, Coelho AL, Peng X, Gulati M, Crestani B, et al. Antifibrotic role of vascular endothelial growth factor in pulmonary fibrosis. *JCI Insight* 2017;2(16).

34. Thomas KA. Fibroblast growth factors. *FASEB J* 1987;1(6):434-440.

35. Shimbori C, Bellaye PS, Xia J, Gauldie J, Ask K, Ramos C, Becerril C, Pardo A, Selman M, Kolb M. Fibroblast growth factor-1 attenuates TGF-β1-induced lung fibrosis. *J Pathol* 2016;240(2):197-210.

36. Guzy RD, Stoilov I, Elton TJ, Mecham RP, Ornitz DM. Fibroblast growth factor 2

is required for epithelial recovery, but not for pulmonary fibrosis, in response to bleomycin. *Am J Respir Cell Mol Biol* 2015;52(1):116-128.

37. Sato S, Goto H, Morizumi S, Okazaki H, Chen Y, Kawano J, Toyoda Y, Hanibuchi M, Azuma M, Nishioka Y. Effect of blockade of fibroblast growth factor receptor signaling in experimental pulmonary fibrosis in mice. *Am J Respir Crit Care Med* 2016;193:A4028.

38. Kim KK, Sisson TH, Horowitz JC. Fibroblast growth factors and pulmonary fibrosis: It's more complex than it sounds. *J Pathol* 2017;241(1):6-9.

39. Joannes A, Brayer S, Besnard V, Marchal-Somme J, Jaillet M, Mordant P, Mal H, Borie R, Crestani B, Mailleux AA. FGF9 and FGF18 in idiopathic pulmonary fibrosis promote survival and migration and inhibit myofibroblast differentiation of human lung fibroblasts in vitro. *Am J Physiol Lung Cell Mol Physiol* 2016;310(7):L615-629.

40. Tandon K HF, Ayaub E, Parthasarathy P, Ackermann M, Kolb M, Wollin L, Ask K. Nintedanib attenuates the polarization of profibrotic macrophages through the inhibition of tyrosine phosphorylation on CSF1 receptor. *Am J Respir Crit Care Med* 2017;195:A2397.

41. Fujita H, Miyadera K, Kato M, Fujioka Y, Ochiiwa H, Huang J, Ito K, Aoyagi Y, Takenaka T, Suzuki T, et al. The novel vegf receptor/met-targeted kinase inhibitor TAS-115 has marked in vivo antitumor properties and a favorable tolerability profile. *Mol Cancer Ther* 2013;12(12):2685-2696.

42. Dohi M, Hasegawa T, Yamamoto K, Marshall BC. Hepatocyte growth factor attenuates collagen accumulation in a murine model of pulmonary fibrosis. *Am J Respir Crit Care Med* 2000;162(6):2302-2307.

43. Gazdhar A, Fachinger P, van Leer C, Pierog J, Gugger M, Friis R, Schmid RA, Geiser T. Gene transfer of hepatocyte growth factor by electroporation reduces bleomycin-induced lung fibrosis. *Am J Physiol Lung Cell Mol Physiol* 2007;292(2):L529-536.

44. Mizuno S, Matsumoto K, Li MY, Nakamura T. Hgf reduces advancing lung fibrosis in mice: A potential role for mmp-dependent myofibroblast apoptosis. *FASEB J* 2005;19(6):580-582.

45. Yaekashiwa M, Nakayama S, Ohnuma K, Sakai T, Abe T, Satoh K, Matsumoto K, Nakamura T, Takahashi T, Nukiwa T. Simultaneous or delayed administration of hepatocyte growth factor equally represses the fibrotic

changes in murine lung injury induced by bleomycin. A morphologic study. *Am J Respir Crit Care Med* 1997;156(6):1937-1944.

46. Kamitani S, Yamauchi Y, Kawasaki S, Takami K, Takizawa H, Nagase T, Kohyama T. Simultaneous stimulation with TGF-β1 and TNF-α induces epithelial mesenchymal transition in bronchial epithelial cells. *Int Arch Allergy Immunol* 2011;155(2):119-128.

47. Sullivan DE, Ferris M, Pociask D, Brody AR. Tumor necrosis factor-α induces transforming growth factor-β1 expression in lung fibroblasts through the extracellular signal-regulated kinase pathway. *Am J Respir Cell Mol Biol* 2005;32(4):342-349.

48. Matsubara N, Shitara K, Naito Y, Kuboki Y, Ohno I, Takahashi H, Hideaki Bando TK, Nozomu Fuse, Tomoko Yamazaki, Naoki Hirayama, Hidenori Fujita, Toshirou Nishida, Toshihiko Doi. First-in-human study of TAS-115, a novel oral MET/VEGFR inhibitor, in patients with advanced solid tumors. *J Clin Oncol* 2015;33(15_suppl):2532.

Figure 1

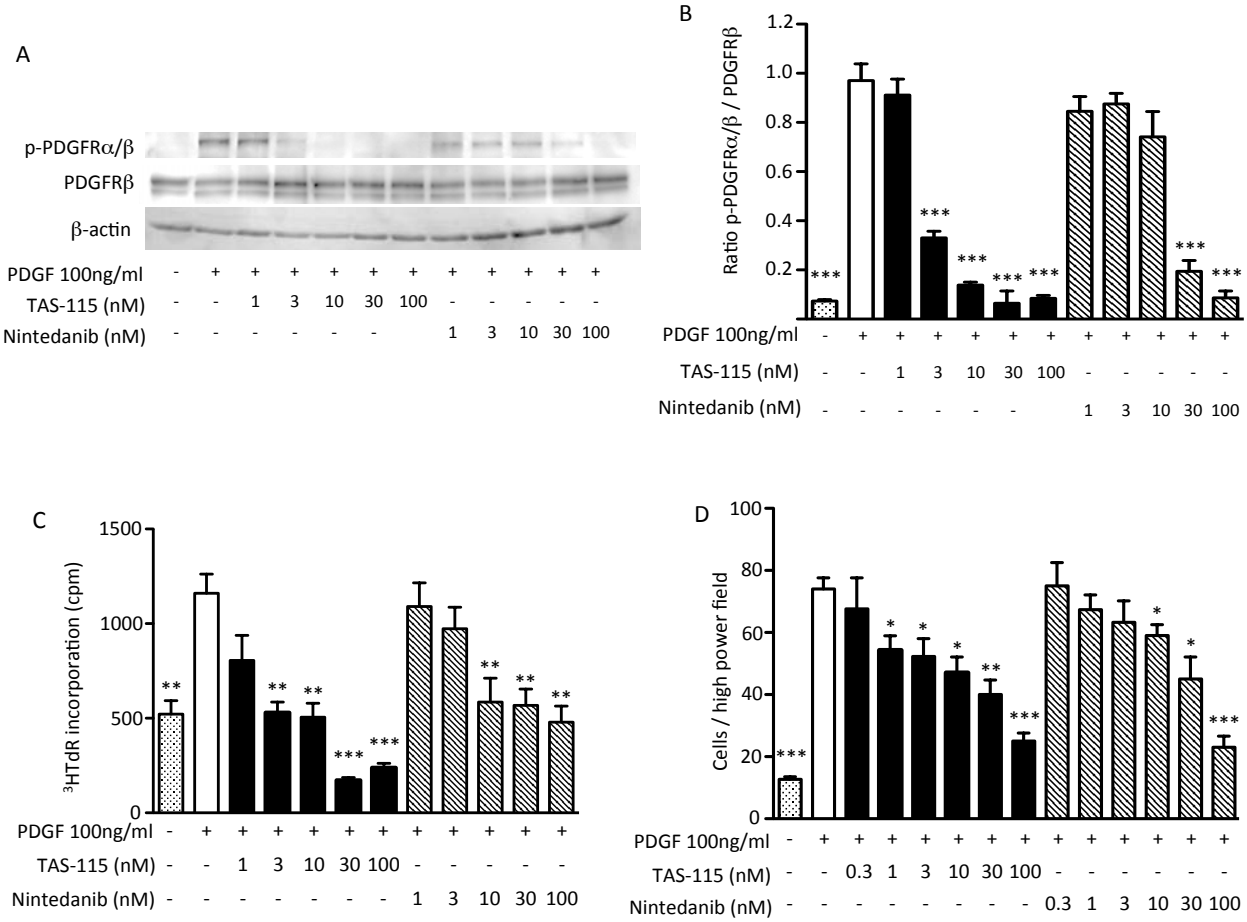
A
p-PDGFRα/β
PDGFRβ
β-actin
PDGF 100ng/ml - + + + + + + + + + + +
TAS-115 (nM) - - 1 3 10 30 100 - - - - -
Nintedanib (nM) - - - - - - 1 3 10 30 100
B
Ratio p-PDGFRα/β / PDGFRβ
1.2
1.0
0.8
0.6
0.4
0.2
***
PDGF 100ng/ml - + + + + + + + + + + +
TAS-115 (nM) - - 1 3 10 30 100 - - - - -
Nintedanib (nM) - - - - - - 1 3 10 30 100
C
³HTdR incorporation (cpm)
1500
1000
500
0
**
***
PDGF 100ng/ml - + + + + + + + + + + +
TAS-115 (nM) - - 1 3 10 30 100 - - - - -
Nintedanib (nM) - - - - - - 1 3 10 30 100
D
Cells / high power field
100
80
60
40
20
0
*
**
***
PDGF 100ng/ml - + + + + + + + + + + + +
TAS-115 (nM) - - 0.3 1 3 10 30 100 - - - - - -
Nintedanib (nM) - - - - - - - 0.3 1 3 10 30 100

Figure 2

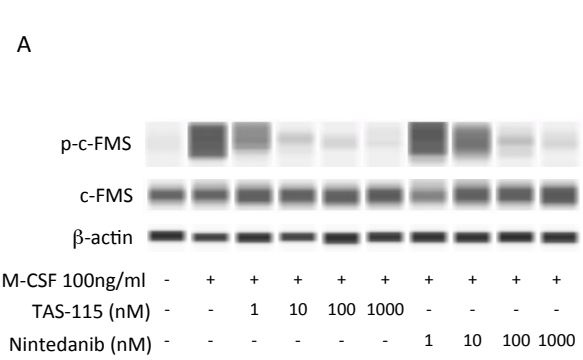
A
p-c-FMS
c-FMS
β-actin
M-CSF 100ng/ml - + + + + + + + + +
TAS-115 (nM) - - 1 10 100 1000 - - - -
Nintedanib (nM) - - - - - - 1 10 100 1000

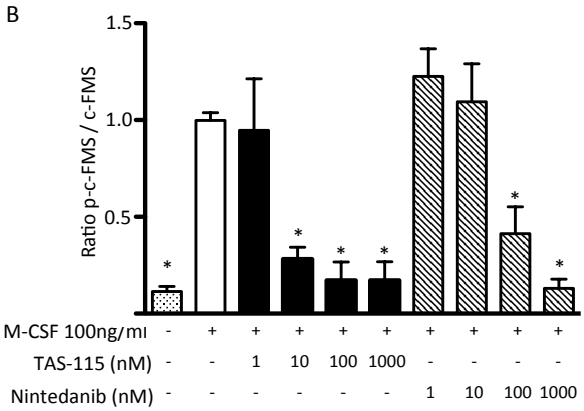
B
Ratio p-c-FMS / c-FMS
1.5
1.0
0.5
*
M-CSF 100ng/ml - + + + + + + + + +
TAS-115 (nM) - - 1 10 100 1000 - - - -
Nintedanib (nM) - - - - - - 1 10 100 1000

Figure 3

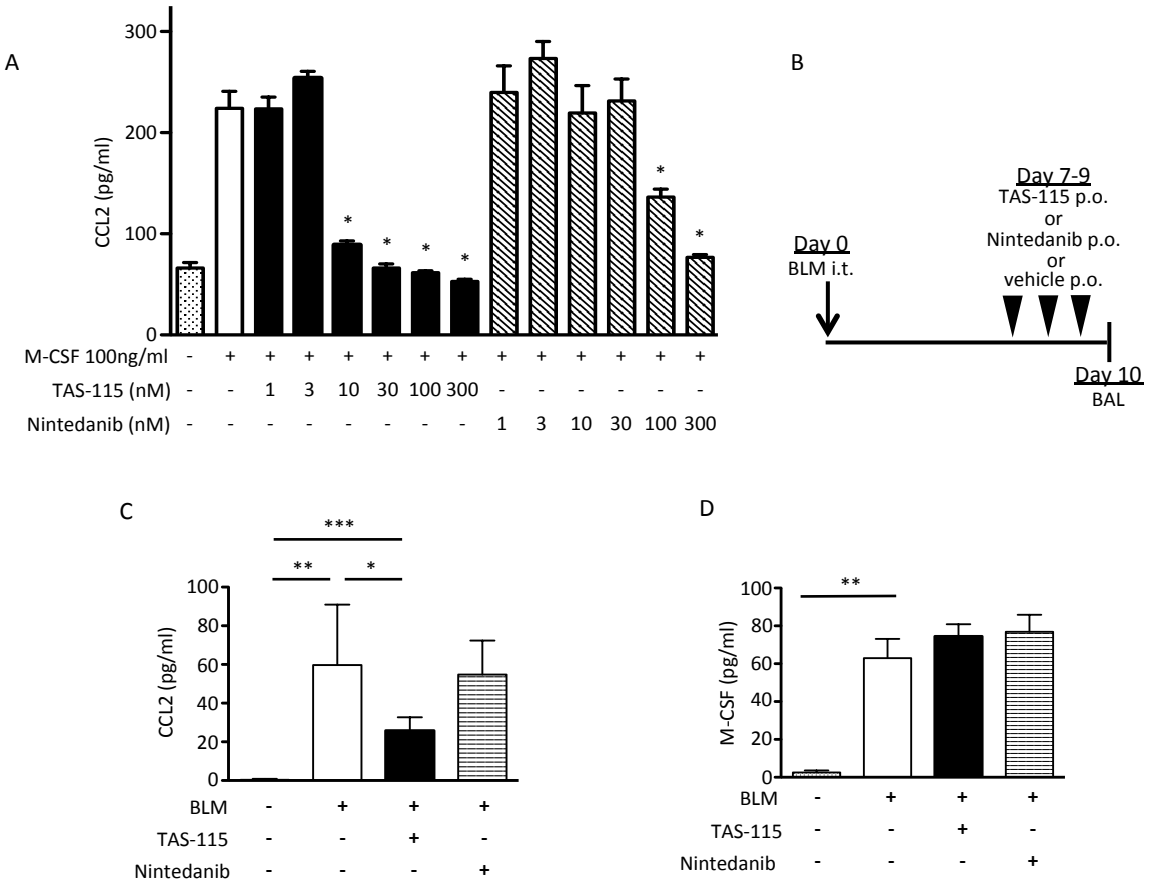
A
CCL2 (pg/ml)
300
200
100
0
M-CSF 100ng/ml - + + + + + + + + + + + + +
TAS-115 (nM) - - 1 3 10 30 100 300 - - - - - -
Nintedanib (nM) - - - - - - - - 1 3 10 30 100 300
B
Day 0
BLM i.t.
Day 7-9
TAS-115 p.o.
or
Nintedanib p.o.
or
vehicle p.o.
Day 10
BAL
C
CCL2 (pg/ml)
100
80
60
40
20
0
***
**
*
BLM - + + +
TAS-115 - - + -
Nintedanib - - - +
D
M-CSF (pg/ml)
100
80
60
40
20
0
**
BLM - + + +
TAS-115 - - + -
Nintedanib - - - +

Figure 4

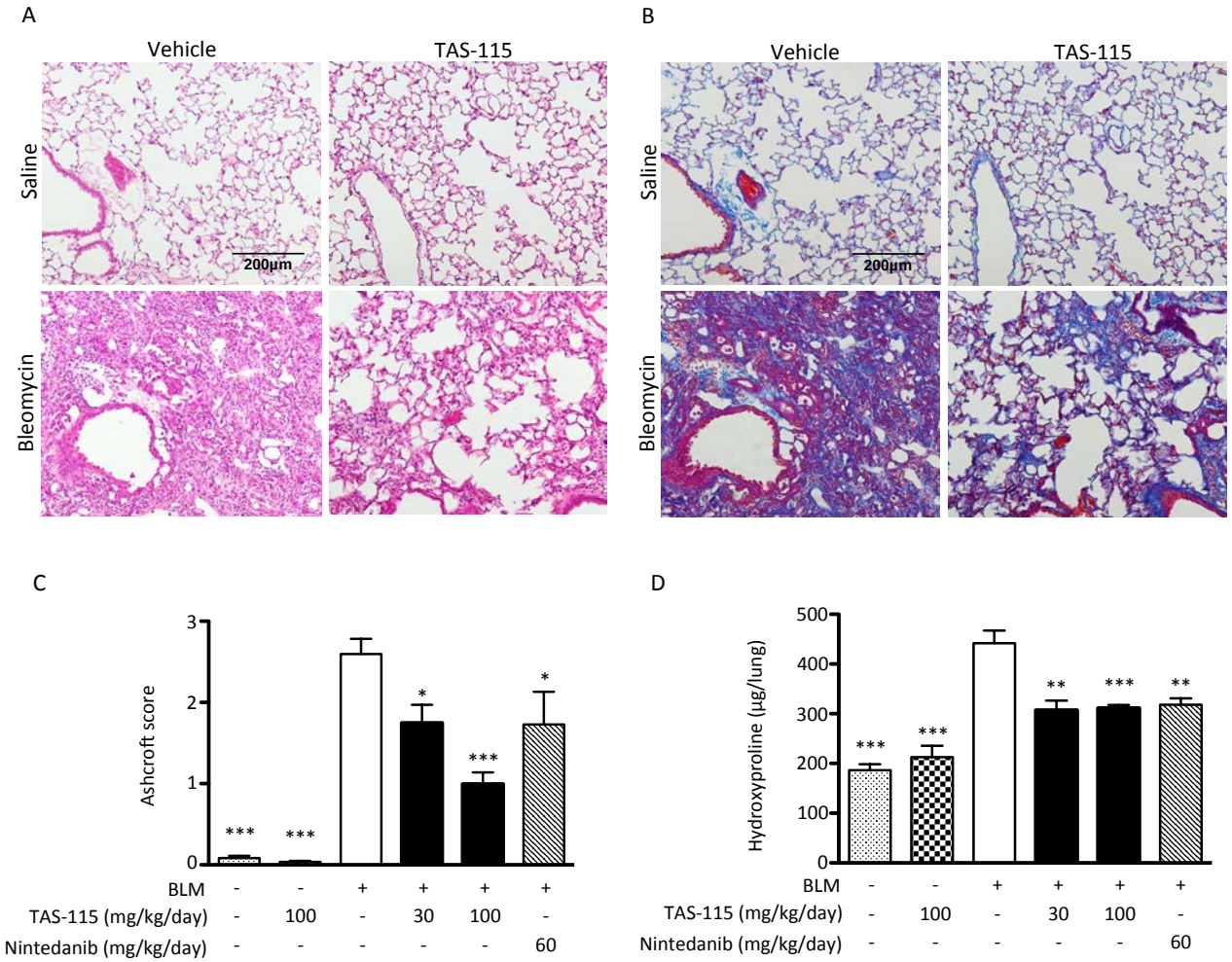
A
Vehicle
TAS-115
Saline
Bleomycin
200μm
B
Vehicle
TAS-115
Saline
Bleomycin
200μm
C
Ashcroft score
0
1
2
3
***
***
*
***
*
BLM - - + + + +
TAS-115 (mg/kg/day) - 100 - 30 100 -
Nintedanib (mg/kg/day) - - - - - 60
D
Hydroxyproline (μg/lung)
0
100
200
300
400
500
***
***
**
***
**
BLM - - + + + +
TAS-115 (mg/kg/day) - 100 - 30 100 -
Nintedanib (mg/kg/day) - - - - - 60

Figure 5

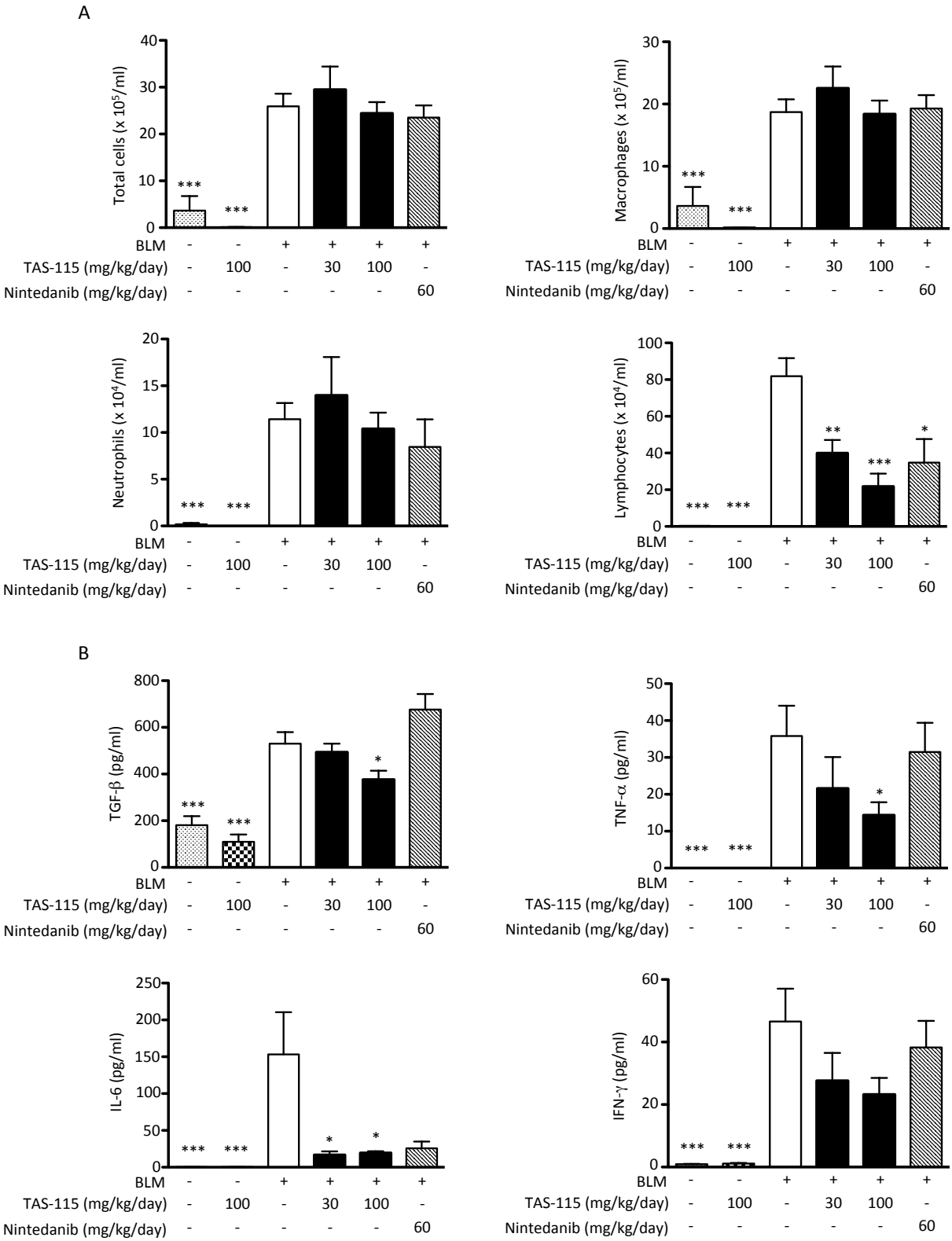
A
Total cells (x 10⁵/ml)
Macrophages (x 10⁵/ml)
Neutrophils (x 10⁴/ml)
Lymphocytes (x 10⁴/ml)
B
TGF-β (pg/ml)
TNF-α (pg/ml)
IL-6 (pg/ml)
IFN-γ (pg/ml)
BLM
TAS-115 (mg/kg/day)
Nintedanib (mg/kg/day)

Novel multiple tyrosine kinase inhibitor TAS-115 attenuates bleomycin-induced pulmonary fibrosis in mice.

Supplementary materials

Mice and agents

Eight-week-old C57BL/6 male mice were purchased from Charles River Japan Inc. (Tokyo, Japan) The mice were maintained in the animal facility of the Tokushima University under specific-pathogen-free conditions according to the guidelines of Tokushima University (1). All experimental protocols were approved by the animal research committee of the University of Tokushima, Japan. TAS-115 was kindly provided by Taiho Pharmaceutical (Tokyo, Japan). Nintedanib was obtained from Chemscene (Monmouth Junction, NJ, USA). Bleomycin (BLM) was purchased from Nippon Kayaku Co. (Tokyo, Japan). Recombinant human cytokines including PDGF-BB, M-CSF and transforming growth factor-β (TGF-β) were purchased from R&D Systems (Minneapolis, MN, USA). Antibodies for PDGFRβ, phosphor-PDGFRα/β, c-FMS, phospho-c-FMS were purchased from Cell Signaling

Technology (Danvers, MA, USA). Anti-collagen 1 antibody was purchased from Abcam (Cambridge, MA, USA). Anti-α smooth muscle actin (α–SMA) antibody was purchased from Sigma-Aldrich (St. Louis, MO, USA). Anti-actin β was purchased from Santa Cruz Biotechnology (Santa. Cruz, CA, USA). Human lung fibroblast cell line MRC-5 cells was purchased from DS PHARMA BIOMEDICAL (Osaka, Japan). Murine lung fibroblasts were isolated according to the method reported previously (2). Fibroblasts were maintained in DMEM medium supplemented with 10% fetal bovine serum (FBS), penicillin (100 U/ml) and streptomycin (50 µg/ml). Bone marrow-derived macrophages (BMDMs) were obtained from male mice. To isolate bone marrow cell suspensions, mice were killed, and their femurs were flushed with RPMI 1640 medium. The collected cells were incubated in RPMI with 2% FBS and 20 ng/ml M-CSF for 5-6 days to allow for their differentiation. Fresh M-CSF was added every 2 days (3). All cells were cultured at 37 °C in a humidified atmosphere of 5% CO_2 in air.

Half maximal inhibitory concentration (IC_{50})

The method of the kinase assay using MET (Carna Bioscience, Inc., Hyogo, Japan) and vascular endothelial growth factor receptor (VEGFR) 2 kinase (Upstate Biotechnology, Lake Placid, NY, USA) was previously described (4).

The kinase assay using fibroblast growth factor receptor (FGFR) 1-4, VEGFR1, PDGFRα and PDGFRβ kinase (Carna Bioscience, Inc.) was conducted using a Mobility Shift Assay. In brief, the assay buffer was prepared from master buffer (20 nmol/L HEPES, 0.01% Triton X-100, pH 7.5) by the addition of DTT (1 nmol/L). The substrate mixture was composed of peptide substrate (CSKtide for FGFR1-4), ATP and metal salt. Test compound solution, substrate mixture and kinase solution were mixed and then incubated for 1 h at room temperature. The kinase reaction was stopped by the addition of EDTA. The reaction mixture was applied to LabChip^{TM} EZ Reader II Screening System, and the product and substrate peptide peaks were quantitated. The kinase reaction was evaluated by the conversion (%), which was calculated from the peak heights of the product (P) and substrate (S) peptides as follows:

Conversion (%) = [P / (P+S)] × 100

The readout values of positive reaction control (complete reaction mixture [Enzyme(+)]) and background(Enzyme[-]) were set as 0% and 100% inhibition, respectively, and the percent inhibition of each test solution was calculated. The IC_{50} value was calculated from the concentration vs. %inhibition curve by fitting to a four-parameter logistic curve.

The experiment was performed three times. The mean IC_{50} value and standard deviation were determined based on three IC_{50} values.

Analyses of the phosphorylation of the receptors

Fibroblasts were cultured in DMEM with PDGF-BB (10 ng/ml) for 15 minutes after incubation with DMEM and various concentrations (0-1000 nM) of TAS-115 or nintedanib for 2 h. To confirm the phosphorylation of PDGFRα/β, these cell were lysed and used for immunoblotting as described previously (5).

BMDMs were cultured in RPMI with M-CSF (100 ng/ml) for 1 minute after incubation with DMEM and various concentrations (0-1000 nM) of TAS-115 or nintedanib for 2 h. After stimulation with MCSF, BMDMs were lysed immediately, and

the phosphorylation of c-FMS was determined using the Simple Western^{TM} System (ProteinSimple, Santa Clara, CA, USA) according to a previous report (6).

Whole-cell extracts were prepared with M-PER reagents (Thermo Fisher Scientific, Waltham, MA, USA) containing phosphatase and protease inhibitor cocktails (Roche, Basel, Switzerland).

Analyses of the expression of the collagen 1 and α–SMA

MRC-5 cells were cultured in DMEM with or without TGF-β (10 ng/ml), PDGF-BB (100ng/ml), TAS-115 (300nM) or nintedanib (300nM). To evaluate the mRNA expression of *COL1A1* or *a-SMA*, cells were incubated for 12 h or 24 h, respectively, and these cells were lysed and used for RT-PCR analysis as described below. To assess the protein expression of collagen 1 or α–SMA, cells were cultured for 24 h or 48 h, respectively, and these cells were lysed and used for immunoblotting described below.

Western blotting

Whole-cell extracts of cells were prepared with M-PER reagents (Thermo Fisher Scientific, Waltham, MA, USA) containing phosphatase and protease inhibitor cocktails (Roche, Basel, Switzerland).

Protein concentrations were measured using the Bradford method. The same amounts of total cell extracts proteins were electrophoresed on 10% NuPAGE Bis-Tris Mini Gels. Gel proteins were then electrophoretically transferred onto polyvinylidene difluoride membranes (Millipore, Billerica, MA, USA) using the WSE-4040 HorizeBLOT 4M-R system (ATTO, Tokyo, Japan). The membrane was treated with Blocking One (Nacalai Tesque, Kyoto, Japan) for 1 h and incubated at 4 °C overnight with primary antibodies. Following four washes, the membrane was incubated with horseradish peroxidase-conjugated secondary antibodies (GE Healthcare, Fairfield, CT, USA) in buffer at room temperature for 1 h. The membrane was washed and developed using Amersham ECL Western Blotting Detection Reagents (GE Healthcare), and the signals were detected using an enhanced chemiluminescence system (GE Healthcare). The intensity of the bands was quantified using the public domain National Institutes of Health imaging program (W.

Rasband, Research Service Branch, National Institutes of Health, Bethesda, MD, USA).

Simple Western™ System

Whole-cell extracts were prepared with M-PER reagents (Thermo Fisher Scientific) containing phosphatase and protease inhibitor cocktails (Roche).

Protein concentrations were measured using the Bradford method. The same amounts of total cell extracts proteins were used for the Simple Western™ System (ProteinSimple, Santa Clara, CA, USA). We used the Simple Western™ System as described in a previous report (6) and according to the manufacturer's instructions, and we analyzed the protein amounts based on the signal intensity.

Cell proliferation assay

Fibroblasts (1×10^4 cells/well) were seeded onto a 96-well plate and cultured in DMEM with PDGF-BB (100 ng/ml) and the indicated concentrations of TAS-115 or nintedanib (0-100 nM) for 72 h. [^{3}H] thymidine deoxyribose (^{3}H-TdR; 1 μCi/well) was

pulsed for the final 18 h, and the incorporation of ^{3}H-TdR was measured using a liquid scintillation counter (7).

Cell migration assay

The migration assay was performed using cell culture inserts with a pore size of 8 μm (BD Biosicence, San Jose, CA, USA). Fibroblasts in DMEM containing 0.1% of FBS were plated to the upper chamber of cell culture inserts with a pore size of 8 μm in the presence or absence of various concentrations of TAS-115 or nintedanib (0-100 nM). PDGF-BB (100 ng/ml) was added to the lower chamber. After 24-h incubation, fibroblasts that had migrated to the bottom surface of the filter were stained with Diff-Quick (Baxter, Miami, FL, USA) and counted in 5 randomly selected fields on each filter under a microscope at 200x magnification. All experiments were performed in triplicate.

qRT-PCR

RT-PCR was performed as previously described (18). Total RNA was extracted from MRC-5 using an RNeasy Mini Kit (Qiagen, Valencia, CA), and was

reverse-transcribed to cDNA using a High Capacity cDNA Reverse Transcription Kit (Applied Biosystems, Carlsbad, CA) according to the manufacturer's instructions. RT-PCR was performed using the CFX96 real-time PCR system (Bio-Rad, Hercules, CA) and the SYBR Premix Ex Taq (TAKARA, Kyoto, Japan). Human *GAPDH* mRNA was used as housekeeping genes, and quantification was performed using the ΔΔ Ct method. The sequences of primers were as follows: *Col1a1* forward, 5'-TCTGCGACAACGGCAAGGTG-3', *Col1a1* reverse, 5'-GACGCCGGTGGTTTCTTGGT-3', *aSMA* forward, 5'-GAGCGTGGCTATTCCTTCGT-3', *aSMA* reverse, 5'-GCCCATCAGGCAACTCGTAA-3', *GAPDH* forward, 5'-GAAGGTGAAGGTCGGAGTC-3', *GAPDH* reverse, 5'-GAAGATGGTGATGGGATTTC-3'.

M-CSF-stimulated CCL2 production by BMDMs

BMDMs (1×10^4 cells/well) were seeded onto a 96-well plate and cultured in DMEM with M-CSF (100 ng/ml) and the indicated concentrations of TAS-115 or nintedanib

(0-100 nM) for 24 h. Supernatants were collected and measured using an ELISA kit (R&D Systems).

Bleomycin-induced pulmonary fibrosis in mice

Mice received a single transbronchial instillation of 3.0 mg/kg BLM on day 0 as previously described (7). TAS-115 (30 or 60 mg/kg), nintedanib (100 mg/kg) or distilled water was administered daily by gavage every day. The dosage of TAS-115 was 30mg/kg or 100mg/kg that was determined based on previous study evaluating its anti-tumor effect *in vivo* (9).

Bronchoalveolar lavage

Mice were anesthetized, and a soft cannula was inserted into the trachea. Bronchoalveolar lavage (BAL) was performed from both lungs with saline (1 ml) at various time points. The total cell count of the BAL fluid was determined using Turk staining solution. The BAL fluid was centrifuged, and the cell pellets were re-suspended into saline and then cytospined onto glass slides. These cells were stained with Diff-Quick staining solution (Baxter), and 200 cells were counted for cell

classification (8). Supernatants were collected and their cytokine concentrations were analyzed as described below.

Cytokine concentrations of BAL fluids

The concentrations of CCL2 and M-CSF of BAL fluids and supernatants of cell cultures were examined using the ELISA kit (R&D Systems). The sensitivities of the ELISA kit for CCL2 and M-CSF were 3.9 and 15.6 pg/ml, respectively. Other cytokines were measured using a Bio-Plex assay (Bio-Rad Laboratories, Hercules, CA, USA).

Hydroxyproline assay

Twenty-one days after BLM instillation, the lungs were harvested and homogenized in distilled water, and the hydroxyproline contents were measured using a Bio-vision hydroxyproline assay kit (BioVision, Mount View, CA, USA).

Histopathology

BLM-treated lungs were harvested, fixed in 10% formalin, and embedded in paraffin. Three-micrometer-thick sections were stained with hematoxylin and eosin (H&E) stain or azan Mallory. In the quantitative analysis, a numeric fibrotic scale was used (Ashcroft score) (9). The mean score was considered to be the fibrotic score.

Statistical analyses

The significance of differences was analyzed using the one-way ANOVA, followed by Tukey's multiple-comparison post-hoc test. *p* values of less than 0.05 were considered to be significant. *p* values of less than 0.05 were considered to be significant. Statistical analyses were performed using the GraphPad Prism software program Ver. 6.01 (GraphPad Software Inc., San Diego, CA, USA).

References

1. Aono Y, Nishioka Y, Inayama M, Ugai M, Kishi J, Uehara H, Izumi K, Sone S. Imatinib as a novel antifibrotic agent in bleomycin-induced pulmonary fibrosis in mice. *Am J Respir Crit Care Med* 2005;171(11):1279-1285.

2. Phan SH, Varani J, Smith D. Rat lung fibroblast collagen metabolism in bleomycin-induced pulmonary fibrosis. *J Clin Invest* 1985;76(1):241-247.

3. Baran CP, Opalek JM, McMaken S, Newland CA, O'Brien JM, Jr., Hunter MG, Bringardner BD, Monick MM, Brigstock DR, Stromberg PC, et al. Important roles for macrophage colony-stimulating factor, CC chemokine ligand 2, and mononuclear phagocytes in the pathogenesis of pulmonary fibrosis. *Am J Respir Crit Care Med* 2007;176(1):78-89.

4. Fujita H, Miyadera K, Kato M, Fujioka Y, Ochiiwa H, Huang J, Ito K, Aoyagi Y, Takenaka T, Suzuki T, et al. The novel VEGF receptor/MET-targeted kinase inhibitor TAS-115 has marked in vivo antitumor properties and a favorable tolerability profile. *Mol Cancer Ther* 2013;12(12):2685-2696.

5. Mitani K, Nishioka Y, Yamabe K, Ogawa H, Miki T, Yanagawa H, Sone S. Soluble Fas in malignant pleural effusion and its expression in lung cancer cells.

Cancer Sci 2003;94(3):302-307.

6. Chen JQ, Heldman MR, Herrmann MA, Kedei N, Woo W, Blumberg PM, Goldsmith PK. Absolute quantitation of endogenous proteins with precision and accuracy using a capillary western system. *Anal Biochem* 2013;442(1):97-103.

7. Sato S, Shinohara S, Hayashi S, Morizumi S, Abe S, Okazaki H, Chen Y, Goto H, Aono Y, Ogawa H, et al. Anti-fibrotic efficacy of nintedanib in pulmonary fibrosis via the inhibition of fibrocyte activity. *Respir Res* 2017;18(1):172.

8. Aono Y, Kishi M, Yokota Y, Azuma M, Kinoshita K, Takezaki A, Sato S, Kawano H, Kishi J, Goto H, et al. Role of platelet-derived growth factor/platelet-derived growth factor receptor axis in the trafficking of circulating fibrocytes in pulmonary fibrosis. *Am J Respir Cell Mol Biol* 2014;51(6):793-801.

9. Ashcroft T, Simpson JM, Timbrell V. Simple method of estimating severity of pulmonary fibrosis on a numerical scale. *J Clin Pathol* 1988;41(4):467-470.

Figure legends

Figure E1. TAS-115 inhibits the phosphorylation of PDGFR on primary murine fibroblasts and suppresses PDGF-induced proliferation and migration. (A) Primary murine fibroblasts were incubated with PDGF-BB (100 ng/ml) with or without different concentrations (0-1000 nM) of TAS-115 or nintedanib. The phosphorylation of PDGFR was analyzed by immunoblotting. (B) Relative intensities of the bands of phosphorylated PDGFRα/β to PDGFRβ are shown. The intensities were determined using a National Institutes of Health imaging program (n=3). (C) The proliferation of murine fibroblasts was measured by a ^{3}H-TdR incorporation assay (n=4). Murine fibroblasts were incubated with PDGF-BB (100 ng/ml) with or without the different concentrations (0-100 nM) of TAS-115 or nintedanib. (D) The effect of TAS-115 or nintedanib on the migration of murine fibroblast was investigated by a trans-well migration assay (n=3). Fibroblasts plated on the upper chamber with a pore size of 8 μm were stimulated with PDGF-BB (100 ng/ml) added to the lower chamber. The indicated concentrations of TAS-115 or nintedanib were added to the upper chamber to assess their effect on cell migration. After 24 h, the number of fibroblasts that had migrated to the bottom surface of the filter was counted. *$p<0.05$ versus groups

treated with PDGF-BB without TAS-115 or nintedanib. **p<0.005 versus groups treated with PDGF-BB without TAS-115 or nintedanib. ***p<0.001 versus groups treated with PDGF-BB without TAS-115 or nintedanib.

Figure E2. TAS-115 does not inhibit TGF-β-induced production of collagen 1 and α-SMA. Human lung fibroblast cell line MRC-5 cells were incubated with or without TGF-β (10ng/ml), PDGF-BB (100 ng/ml), TAS-115 (300nM) or nintedanib (300nM). (A)(B) Comparison of the mRNA expression in MRC-5 cells. After 12 h (A) or 24 h (B) incubation, mRNA expression of *COL1A1* (A) and *α-SMA* (B) was analyzed by RT-PCR. *p<0.05 versus groups treated with TGF-β without PDGF-BB, TAS-115 or nintedanib. (C)(D) Immunoblotting showing the expression of collagen 1 (C) and α-SMA (D). MRC-5 cells were incubated for 24 h (C) or 48 h (D).

Figure E3. TAS-115 treatment affects the cell counts (A) and the expression of inflammatory cytokines (B) in the BALF of BLM-treated mice. Mice received a single transbronchial instillation of 3.0 mg/kg BLM on day 0, and TAS-115 (30 or 100 mg/kg/day), nintedanib (60 mg/kg/day) or vehicle was administered daily from day 0.

Mice were killed, and the BALFs were collected on day 7 (n=6). Concentrations of TNF-α and IFN-γ on day7 were undetectable. *p<0.001 versus groups treated with BLM without TAS-115 or nintedanib.

Figure E4. TAS-115 treatment affects the cell counts (A) and the expression of inflammatory cytokines (B) in the BALF of BLM-treated mice. Mice received a single transbronchial instillation of 3.0 mg/kg BLM on day 0, and TAS-115 (30 or 100 mg/kg/day), nintedanib (60 mg/kg/day) or vehicle was administered daily from day 0. Mice were killed, and the BALFs were collected on day 21 (n=6). *p<0.05 versus groups treated with BLM without TAS-115 or nintedanib. **p<0.01 versus groups treated with BLM without TAS-115 or nintedanib. ***p<0.001 versus groups treated with BLM without TAS-115 or nintedanib.

Figure E1

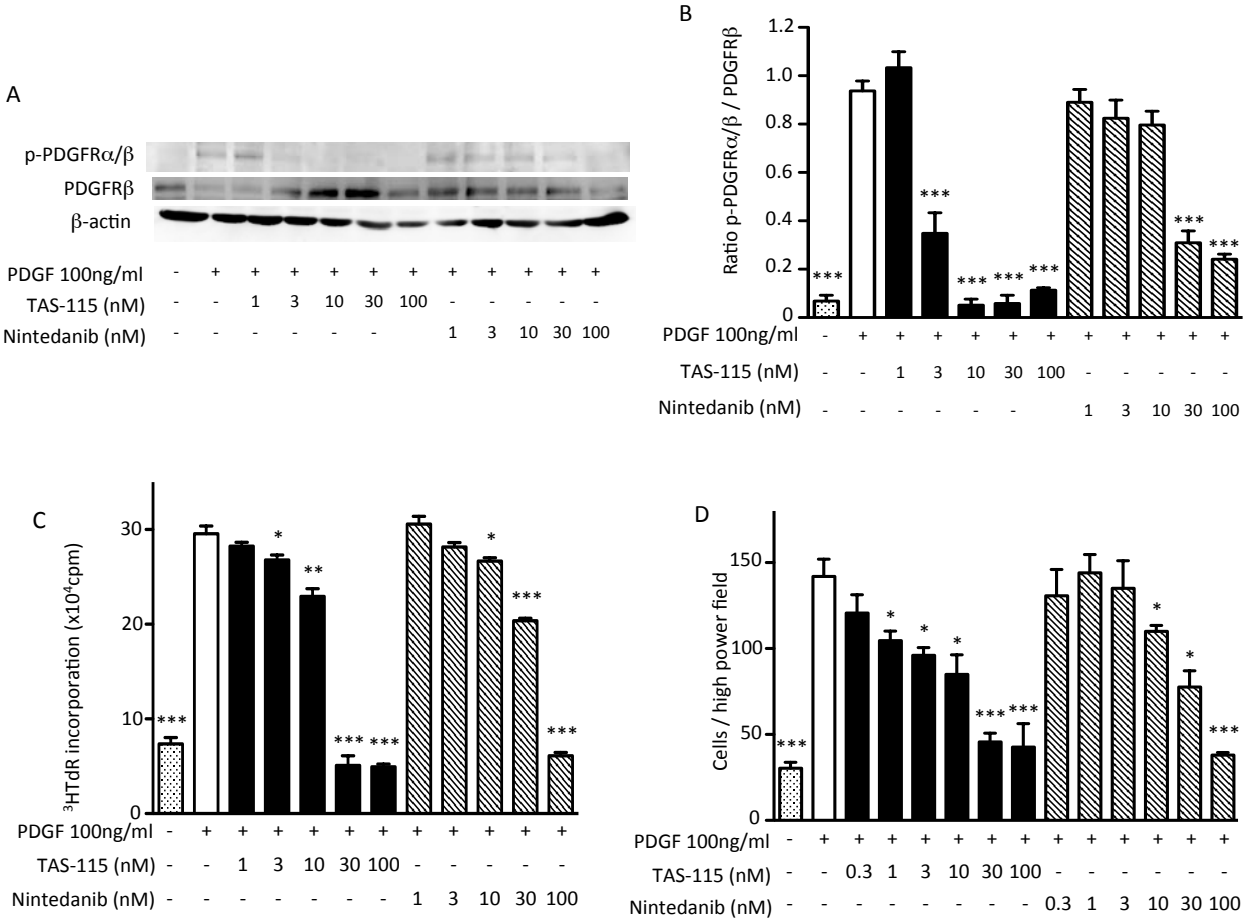
A
p-PDGFRα/β
PDGFRβ
β-actin
PDGF 100ng/ml - + + + + + + + + + + +
TAS-115 (nM) - - 1 3 10 30 100 - - - - -
Nintedanib (nM) - - - - - - 1 3 10 30 100
B
Ratio p-PDGFRα/β / PDGFRβ
1.2
1.0
0.8
0.6
0.4
0.2
0
***
PDGF 100ng/ml - + + + + + + + + + + +
TAS-115 (nM) - - 1 3 10 30 100 - - - - -
Nintedanib (nM) - - - - - - 1 3 10 30 100
C
³HTdR incorporation (x10⁴cpm)
30
20
10
0
*
**
***
PDGF 100ng/ml - + + + + + + + + + + +
TAS-115 (nM) - - 1 3 10 30 100 - - - - -
Nintedanib (nM) - - - - - - 1 3 10 30 100
D
Cells / high power field
150
100
50
0
*
***
PDGF 100ng/ml - + + + + + + + + + + + +
TAS-115 (nM) - - 0.3 1 3 10 30 100 - - - - - -
Nintedanib (nM) - - - - - - - 0.3 1 3 10 30 100

Figure E2

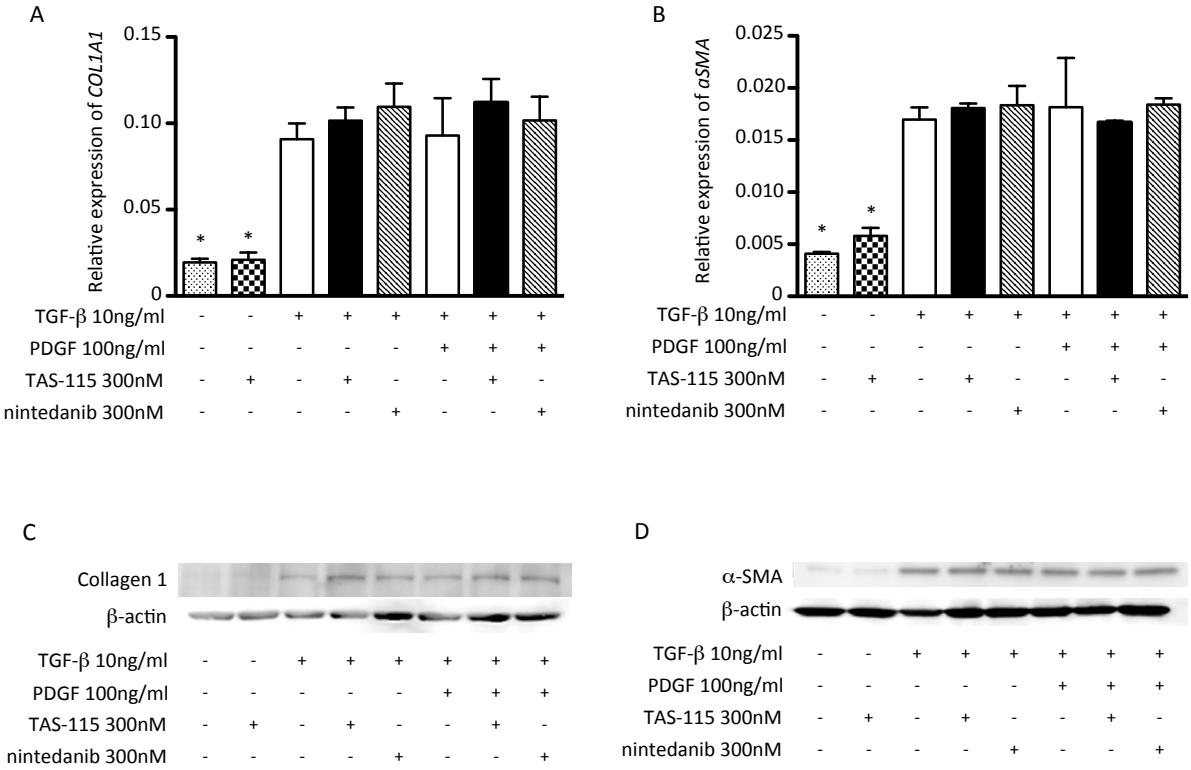
A
Relative expression of COL1A1
0.15
0.10
0.05
0
B
Relative expression of αSMA
0.025
0.020
0.015
0.010
0.005
0
TGF-β 10ng/ml
PDGF 100ng/ml
TAS-115 300nM
nintedanib 300nM
C
Collagen 1
β-actin
D
α-SMA
β-actin

Figure E3

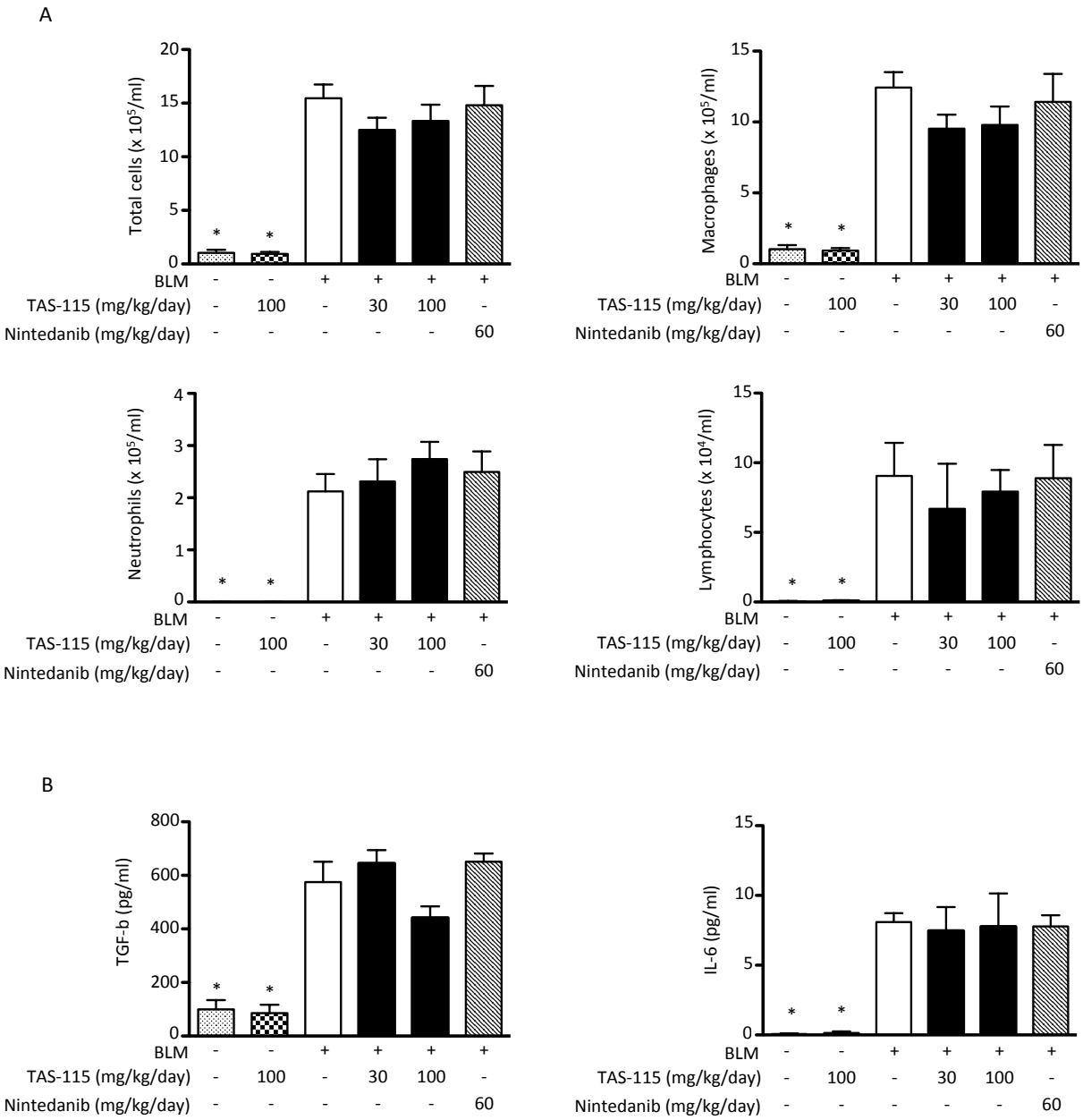
A
Total cells (x 10⁵/ml)
Macrophages (x 10⁵/ml)
Neutrophils (x 10⁵/ml)
Lymphocytes (x 10⁴/ml)
BLM
TAS-115 (mg/kg/day)
Nintedanib (mg/kg/day)
B
TGF-b (pg/ml)
IL-6 (pg/ml)

Figure E4

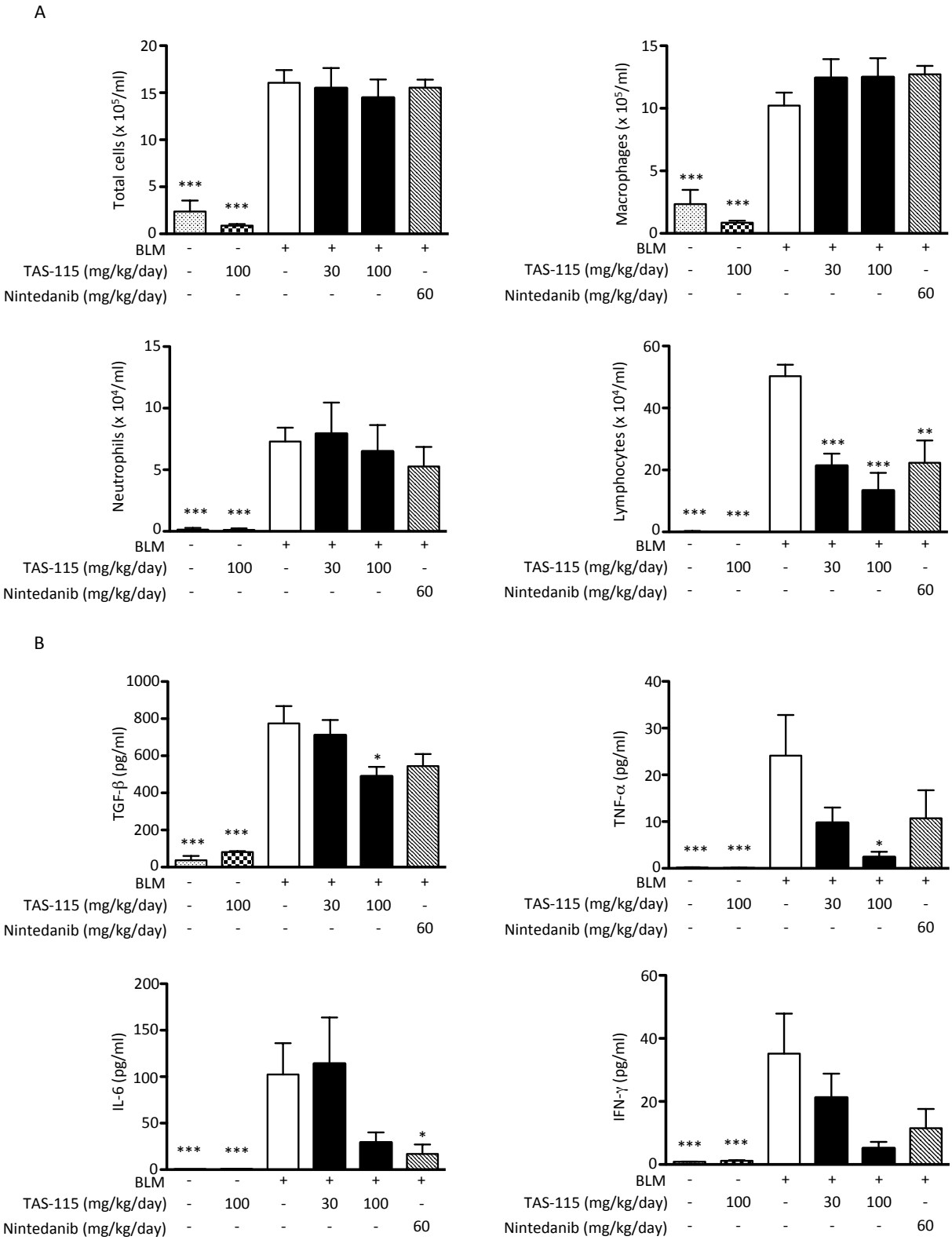
A
Total cells (x 10⁵/ml)
Macrophages (x 10⁵/ml)
Neutrophils (x 10⁴/ml)
Lymphocytes (x 10⁴/ml)
B
TGF-β (pg/ml)
TNF-α (pg/ml)
IL-6 (pg/ml)
IFN-γ (pg/ml)
BLM
TAS-115 (mg/kg/day)
Nintedanib (mg/kg/day)